



Published in final edited form as:

Mol Pharm. 2014 July 7; 11(7): 2022–2029. doi:10.1021/mp500054h.

Validating anti-metastatic effects of natural products in an engineered microfluidic platform mimicking tumor microenvironment

Yiming Niu^{1,‡}, Jing Bai^{2,3,‡}, Roger D. Kamm^{2,3}, Yitao Wang^{1,*}, and Chunming Wang^{1,*}

¹State Key Laboratory of Quality Research in Chinese Medicine, Institute of Chinese Medical Sciences, University of Macau, Avenida Padre Tomas Pereira, Taipa, Macao SAR, China

²BioSystems and Micromechanics IRG, Singapore-MIT Alliance for Research and Technology (SMART) Center, 1 CREATE Way, #04-13/14 Enterprise Wing, Singapore 138602, Singapore

³Department of Biological Engineering and Department of Mechanical Engineering, Massachusetts Institute of Technology, Cambridge, MA 02139, USA

Abstract

Development of new, anti-metastatic drugs from natural products has been substantially constrained by the lack of a reliable *in vitro* screening system. Such a system should ideally mimic the native, three-dimensional (3D) tumor microenvironment involving different cell types and allow quantitative analysis of cell behavior critical for metastasis. These requirements are largely unmet in the current model systems, leading to poor predictability of the *in vitro* collected data for *in vivo* trials, as well as prevailing inconsistency among different *in vitro* tests. In the present study, we report application of a 3D, microfluidic device for validation of the anti-metastatic effects of twelve natural compounds. This system supports co-culture of endothelial and cancer cells in their native 3D morphology as in the tumor microenvironment, and provides real-time monitoring of the cells treated with each compound. We found that three compounds, namely sanguinarine, nitidine, and resveratrol, exhibited significant anti-metastatic or anti-angiogenic effects. Each compound was further examined for its respective activity with separate conventional biological assays, and the outcomes were in agreement with the findings collected from the microfluidic system. In summary, we recommend use of this biomimetic model system as a new engineering tool for high-throughput evaluation of more diverse natural compounds with varying anti-cancer potentials.

Keywords

microfluidics; metastasis; natural products; angiogenesis; cell co-culture

*Corresponding Authors: Chunming Wang (cmwang@umac.mo) and Yitao Wang (ytwang@umac.mo) are at University of Macau, ICMS-Block III, Avenida Padre Tomas Pereira, Taipa, Macau SAR, China.

‡These authors contributed equally.

SUPPORTING INFORMATION

Description of the 12 natural compounds, preparation of the multicellular cancer aggregates (MCAs), *in vitro* angiogenic and scratch assays, and Topoisomerase inhibition assay. This information is available free of charge via the Internet at <http://pubs.acs.org/>.

Metastasis is the spreading of cancer from its primary site to other parts of the body.¹ It is the late, critical stage that accounts for most cancer deaths, and is a main target for the development of anti-cancer drugs.¹ Over the last two decades, a number of compounds derived from natural resources have shown preliminary anti-metastatic potential when tested in cell culture.² However, the drug efficacy data collected from these studies have largely proved difficult to reproduce in other *in vitro* systems or to predict further *in vivo* tests, providing little guidance for downstream investigations including animal studies. Moreover, investigations into the exact mechanisms of these natural compounds appear obscure or inconsistent among one another. Typical examples include studies of berberine and evodiamine, two natural alkaloids with extensive reports for their anti-metastatic function *in vitro*.³ The former's effect was attributed to a long, confusing list of mechanisms, involving inhibition of Akt-nuclear factor kappa B (NF-kappa B)-MMP2/9 cascade^{3a}, activation of AMP-activated protein kinase (AMPK)⁴ and blocking of heparanase expression,⁵ among many others. The latter was suggested to inhibit metastasis in cultured cancer cells,^{3c-e} but was reported elsewhere to effectively increase the secretion of interleukin-8 (IL-8),⁶ a cytokine well-evidenced to promote adhesion, migration and invasion of cancer cells.⁷ As a result, very few of these molecules could finally reach clinical trials.

Among the reasons for the above inconsistencies is the lack of a reliable *in vitro* model for anti-metastatic screening. Metastasis involves dynamic interaction of several cell types residing in a complex, three-dimensional (3D) microenvironment, notably including tumor cells and endothelial cells.^{1b} Therefore, in the screening system, it is essential to maintain the 3D, native morphology of cells, and it is senseless to neglect the crosstalk between endothelial cells and tumor cells. Nevertheless, most present models for *in vitro* screening are simply carcinoma monolayer cultivated in the two-dimensional (2D) tissue-culture plastics (TCPs), without taking into consideration communications between, and proper morphology of, different cell types. Although co-culture techniques such as the Transwell device have increasingly been used in the recent years, they only achieved to physically culture two cell types in one well yet still fail to mimic the 3D morphology – and hence the behavior and phenotypes – of various cells involved. Furthermore, hardly any current model provides real-time monitoring of the behavior of the two (or more) cells types and especially their dynamic interactions, which are crucial given the ample evidence that secretion of one cell type highly influences and even ‘educates’ the others.⁸ All these concerns are providing answers to the inconsistent performances of the natural compounds – their effect on cancer cells in two-dimensional (2D) monolayer may be resisted by the same cells in their native, 3D organization *in vivo*, or their inhibition of cancer cell spreading was probably antagonized by cytokines released from endothelium. Obviously, new models that closely mimic the genuine tumor microenvironment and that can recapitulate part of the complex metastatic process are in high demand.

In our previous study, we reported a microfluidics-based model that highly recapitulates tumor microenvironment by co-culturing endothelial cells in 3D collagen gels and cancer cells formed into 3D spheroids⁹. Model drugs such as Gefitinib (AstraZeneca, Food and Drug Administration-approved) and Masitinib (AB Science, currently undergoing Phase III clinical trial), which had inhibitory effects on epithelial-mesenchymal transition (EMT), a

key mechanism of metastasis, were applied to the device followed by real-time monitoring and quantitative analysis. The outcomes were not only consistent with findings based on conventional *in vitro* and *in vivo* platforms, but also validated the effects of those drugs in inhibiting EMT and thus metastasis with precise range of effective dose and dynamic monitoring throughout the investigation. This kind of tools would be particularly needed for accurate evaluation of natural products. Therefore, in this study, we hypothesized that using such a bio-mimicking system could help to validate the anti-metastatic effects of natural compounds under the specific, co-cultural condition.

We first prepared the microfluidics device. Our principle of design was to introduce collagen gel into particular zones in the device. Endothelial cells should adhere to this gel, spread on the gel, and form an intact endothelial layer. Then, in the same chamber pre-prepared cancer-cell spheroids would be added and co-cultured with the endothelial cells, so as to create a physiologically relevant microenvironment. We fabricated the device using polydimethylsiloxane (PDMS) bound to a glass coverslip to form a transparent chamber; during the process, the PDMS replicas were the negative image of the positive relief structure of patterned wafer made by soft lithography. The entire fabrication followed our previous protocol⁹ with minor modification in device channels in order to better visualize the morphology of the endothelial layer. As discussed later, we would particularly investigate the influence of different compounds on the human umbilical vein endothelial cells (HUVECs). As illustrated in Figure 1A, we added in one channel collagen solution (Type I, rat tail, BD Singapore) which, after gelation, supported the adhesion of endothelial cells (HUVECs, Lonza, Switzerland). Human lung carcinoma cell line A549 (ATCC, USA, CCL-185) stably expressing H2B-mCherry (pH2B-mCherry_IRES_puro2, Addgene® Plasmid 21045, USA), pre-generated through FuGENE 6 transfection (Roche, Singapore), puromycin selection, and FACS sorting, were cultured to form spheroids (40–100 μm in diameter) as described before. These spheroids were collected and mixed in a pre-optimized collagen buffer and pipetted into the designated channel carefully to avoid spillage to the adjacent channel. The average distance between endothelial layer and cancer spheroids defines that in the typical tumor microenvironment which allows sufficient cell-cell communications. The secretion of HUVECs could diffuse into the collagen matrix, along with drug molecules upon the formation of an intact endothelial monolayer. A sample photograph of fluorescently stained cells in this device is shown in Figure 1B.

We tested 12 natural compounds in this system (Figure 1C). We picked them up from a large number of candidates for two reasons – i) they have been reported to inhibit metastasis *in vitro*, and ii) they are representatives for two common structural families of natural products. Any validated bioactivity with these molecules may provide information for study of other compounds in the same categories. Compounds 1 to 6, namely matrine¹⁰, sanguinarine¹¹, harmine¹², nitidine¹³, berberine^{3a, b} and evodiamine^{3c}, are alkaloids. Compounds 7 to 12, which are resveratrol¹⁴, epigallocatechin gallate (EGCG)¹⁵, curcumin¹⁶, quercetin¹⁷, catechin¹⁸ and gallic acid¹⁹, respectively, belong to the polyphenol class. After consulting literature for the half maximal inhibitory concentration (IC_{50}) of each compound against A549 or similar cancer cell lines in 2D condition (Supplementary Table 1), we set a working concentration of 10 μM for Compounds 2 – 8, 50 μM for Compounds 9

– 12, and 100 μM for Compound 1. The compounds were applied to the endothelial channel, resembling the real process of drug diffusion across the capillary vessel in the circulating system. Before spheroid seeding, it was necessary to double check the devices one by one, in order to confirm the endothelial cells were spreading well and forming an intact layer. After spheroid seeding, we needed to check again to ensure both cell types were in their proper morphology..

Two of the twelve tested molecules, Compounds 4 and 7, significantly inhibited metastasis, as revealed by the morphology of A549 spheroids taken at 0 and 36 hours (Figure 2A) and the subsequent quantification of the dispersion (Figure 2B). In brief, for a specific spheroid, we first counted the number of cell nuclei, and then calculated the dispersion by using the Imaris 6.0 software (Bitplane), which generated a 3D histogram of nuclei distribution and helped us figure out the spheroid center (X_c, Y_c, Z_c) as well as the special coordinates of all nuclei (X_n, Y_n, Z_n). We next determined the standard deviation of each nucleus from the spheroid center (σ , of a given spheroid). In doing so, we could evaluate the efficacy of each compound by calculating the normalized dispersion (σ / σ_0), where σ and σ_0 (at 0 h) must be generated from the same device.

Compound 4, or nitidine, almost completely abolished the dispersion of the spheroids, apparently killing the cancer cells, which remains further verification in 2D cultures. In comparison, Compound 7, resveratrol, was less strong yet convincingly effective. It inhibited the dispersion to ~ 60% of blank control. We further tested this compound at 10, 50, 100 and 500 μM , and found that its dose dependency was less obvious at the range between 10 and 100 than from 100 to 500 μM (Figure 2C). Meanwhile in the endothelial channel, Compound 2, sanguinarine, was notable to be the only compound that drastically disrupted endothelial cell layer, according to cell morphology observation and live cell staining (Figure 2D). We assumed that Compound 2 had inhibitory effects specifically on endothelial cells, and it would be worth evaluating its anti-angiogenic potential. Apart from these three molecules, all other samples did not show statistically significant inhibition of spheroids dispersion or any obvious influence on endothelial cells. Although it was inappropriate to exclude their anti-metastatic or anti-angiogenic potential at all purely based on these tests, we do not recommend set priority of further evaluation on these 9 compounds. Instead, we focused on Compounds 2, 4, and 7, whose interesting performance in the device motivated us to pick them up for further exploration in cultured plates.

We examined the cytotoxicity of Compound 2 on the two cell types cultured on TCPS with MTT assay. It was shown that HUVECs were more sensitive than A549 to this molecule at a lower dose (Figure 3A), which was consistent with our finding in the microfluidic device. However, Compound 2 at a higher dose of 5.44 μM , which was still lower than the tested dose in the device, almost completely killed both cell types, revealing the A549 cells were more sensitive to the drug in 2D monolayer than in 3D spheroids. We further examined its anti-angiogenic potential with tube formation assay on Matrigel (BD Bioscience, USA) supplemented with basic fibroblast growth factor (bFGF). After 8 h of treatment, compound 2 could effectively inhibit tube formation at a concentration as low as 0.68 μM (~35% inhibition) and abolish all capillary-like tubes at 2.72 μM (Figure 3B). Hence, our findings both in and out of the device validated the anti-angiogenic effects of sanguinarine²⁰, and for

the first time recommended a relatively lower concentration, 2.72 μM , for future evaluation of specific, anti-angiogenic compounds. At this concentration, the compound showed strong anti-angiogenic effects but low toxicity to A549 cells. On the contrary, several other compounds, including Compounds 3 (harmine),¹² 4 (nitidine),²¹ 5 (berberine),²² 7 (resveratrol),²³ 10 (quercetin)²⁴ and 12 (gallic acid),²⁵ have been reported to be anti-angiogenic in conventional cultures but failed to be validated in this co-culture system, though in this study we had chosen a concentration for each compound that is close to its own IC_{50} against HUVECs.

Compound 4 was tested at a wide range of concentration (1.63 to 26.05 μM) for its cytotoxicity, showing moderate inhibition on the viability of both cell types (Figure 4A). Its effect on A549 cells in monolayer appeared relatively mild as compared with that in the device. However, this might be due to the different cell behavior in 2D and 3D. As such, we generated the A549 spheroids again on polystyrene surface treated with 0.2% pluronic (Pluronic F108, BASF) for 4 days.²⁶ Live/Dead staining indicated that the cell viability was extremely decreased by the treatment of Compound 4 (Figure 4B), which was consistent with the finding in the device and confirmed our assumption that these cancer cells had distinct sensitivity in 2D and in 3D organization. Furthermore, because this molecule was reported to induce cell death via inhibition of topoisomerase inhibitor, we examined how it affected topoisomerase I in cleaving plasmid DNA. Agarose gel electrophoresis clearly indicated that nitidine in all three tested concentrations (13, 26 and 52 μM) could unwind the supercoiled DNA, and the intensity of 'relaxed' DNA appeared to have a positive correlation with the compound dose (Figure 4C). Therefore, we suggest that Compound 4, regardless of its effects against metastasis, is effective in inducing cell apoptosis via inhibition of topoisomerase, which may be the starting point for future trials aimed at understanding the cellular mechanism of nitidine.

We next evaluated the anti-metastatic effect of Compound 7. This compound was of minimal toxicity to either cell type even at a considerably high concentration (109.53 μM for HUVECs and 219.07 for A549, respectively) (Figure 5A), but its inhibitory effect on the migration of A549 cancer cells was proved with scratch wound assay, followed by morphology observation (Figure 5B) and measurement of the average width between the two edges of each wound (Figure 5C). The average migration rate of PMA-challenged cells, which had been stimulated from 1.82 to 3.97 μm per hour, was effectively decreased to 3.38 and a remarkable 1.77 μm per hour by resveratrol at the doses of 13.5 μM and 27 μM , respectively (Supplementary Table 2, with the calculation method). Such findings, in combination with the observations in the device, highlight that this compound possesses both potent anti-metastatic activity and minimal cytotoxicity at a very reasonable dose. Moreover, we speculate that its activity is associated with inhibition of EMT in cancer cells, according to the previous application of this platform.⁹ However, extensive experiments including staining of specific epithelial markers (such as E-cadherin)²⁷ and mesenchymal markers (such as vimentin)²⁸ are required before making further conclusion.

As presented, we have picked up three compounds – sanguinarine, nitidine and resveratrol – for their intriguing performance in the microfluidic system, and verified their different activities accordingly with tailor-made experiments out of device. For each compound, the

good correlation between its on- and off-chip performances was of major interest to us. As a drug screening platform in general, this system has shown potential to be a reliable and efficient tool for high-throughput compound screening. As an anti-metastatic model, its recapitulation of native microenvironment and real-time quantitative analysis provide reliable information taking into consideration of various biochemical and biophysical factors such as cell-cell communication, cytokine diffusion and/or cell morphology. Meanwhile, for the other nine compounds, it is neither the conclusion nor the aim of this study to assume that these molecules have no anti-metastatic effect. They failed to outperform Compounds 2, 4 and 7 at the given dose (though having taken reference from literature about their IC₅₀) to a specific cell line in this particular system, and were therefore not prioritized for the subsequent cell biology tests. However, they might be potent to different cancer cells via different mechanisms in another system, which requires fine tuning to the current device to introduce new biological microenvironment. Fortunately, the present microfluidic device is an open platform, readily fabricated with well-established techniques and conveniently adjustable to create different cell conditions.²⁹ We are confident in preparation of new, on-demand systems for validation of diverse natural molecules with specific therapeutic potentials.

To summarize, we have for the first time validated the anti-metastatic effects of natural compounds in an engineered platform. This 3D, microfluidics based system mimicking tumor microenvironment allows quantitative monitoring of endothelial and cancer cells in their native 3D organization. Of the selected 12 molecules, three compounds exhibited interesting but different activities within the given dose range, which were further verified with separate assays performed out of the device. Such findings may provide important insights on selection of biological targets and models in future, comprehensive investigations. More specifically, we would recommend testing Compound 2 for its anti-angiogenic potential in relevant models, exploring Compound 4 for its exact mechanism of inducing apoptosis, as well as trialing Compound 7 as a potent inhibitor of EMT in various cancer models *in vivo*.

Supplementary Material

Refer to Web version on PubMed Central for supplementary material.

Acknowledgments

This study was supported in part by grants from the Macao Science and Technology Development Fund (FDCT/077/2011/A3) to Y.W. and (FDCT/116/2012/A) to C.W. The authors thank Prof Jinjian Lu at the Institute of Chinese Medical Sciences, University of Macau, for sharing reagents for the angiogenic assay, and all technicians at this institute for their excellent technical assistance.

References

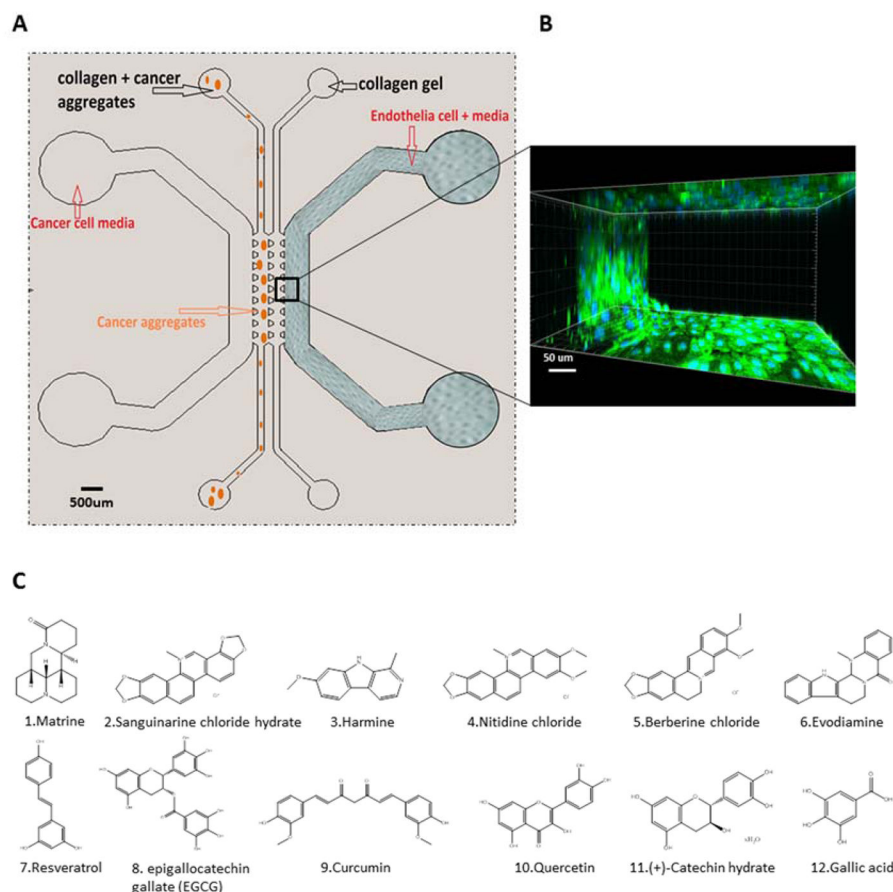
1. (a) Reymond N, d'Agua BB, Ridley AJ. Crossing the endothelial barrier during metastasis. *Nat Rev Cancer*. 2013; 13(12):858–70. [PubMed: 24263189] (b) Quail DF, Joyce JA. Microenvironmental regulation of tumor progression and metastasis. *Nat Med*. 2013; 19(11):1423–37. [PubMed: 24202395]
2. (a) Bhatnagar I, Thomas NV, Kim SK. Natural flora and anticancer regime: milestones and roadmap. *Anticancer Agents Med Chem*. 2013; 13(6):910–22. [PubMed: 23293884] (b) Ali R,

Mirza Z, Ashraf GM, Kamal MA, Ansari SA, Damanhour GA, Abuzenadah AM, Chaudhary AG, Sheikh IA. New anticancer agents: recent developments in tumor therapy. *Anticancer Res.* 2012; 32(7):2999–3005. [PubMed: 22753764] (c) Mehta RG, Murillo G, Naithani R, Peng X. Cancer chemoprevention by natural products: how far have we come? *Pharm Res.* 2010; 27(6):950–61. [PubMed: 20238150]

3. (a) Kuo HP, Chuang TC, Tsai SC, Tseng HH, Hsu SC, Chen YC, Kuo CL, Kuo YH, Liu JY, Kao MC. Berberine, an isoquinoline alkaloid, inhibits the metastatic potential of breast cancer cells via Akt pathway modulation. *J Agric Food Chem.* 2012; 60(38):9649–58. [PubMed: 22950834] (b) Tillhon M, Guaman Ortiz LM, Lombardi P, Scovassi AI. Berberine: new perspectives for old remedies. *Biochem Pharmacol.* 2012; 84(10):1260–7. [PubMed: 22842630] (c) Du J, Wang XF, Zhou QM, Zhang TL, Lu YY, Zhang H, Su SB. Evodiamine induces apoptosis and inhibits metastasis in MDAMB-231 human breast cancer cells in vitro and in vivo. *Oncol Rep.* 2013; 30(2): 685–94. [PubMed: 23708383] (d) Jiang J, Hu C. Evodiamine: a novel anti-cancer alkaloid from *Evodia rutaecarpa*. *Molecules.* 2009; 14(5):1852–9. [PubMed: 19471205] (e) Ogasawara M, Matsunaga T, Takahashi S, Saiki I, Suzuki H. Anti-invasive and metastatic activities of evodiamine. *Biol Pharm Bull.* 2002; 25(11):1491–3. [PubMed: 12419968]
4. Park JJ, Seo SM, Kim EJ, Lee YJ, Ko YG, Ha J, Lee M. Berberine inhibits human colon cancer cell migration via AMP-activated protein kinase-mediated downregulation of integrin beta1 signaling. *Biochem Biophys Res Commun.* 2012; 426(4):461–7. [PubMed: 22943849]
5. Yan L, Yan K, Kun W, Xu L, Ma Q, Tang Y, Jiao W, Gu G, Fan Y, Xu Z. Berberine inhibits the migration and invasion of T24 bladder cancer cells via reducing the expression of heparanase. *Tumour Biol.* 2013; 34(1):215–21. [PubMed: 23065570]
6. Shi HL, Wu XJ, Liu Y, Xie JQ. Berberine counteracts enhanced IL-8 expression of AGS cells induced by evodiamine. *Life Sci.* 2013; 93(22):830–9. [PubMed: 24063987]
7. (a) Inoue K, Slaton JW, Kim SJ, Perrotte P, Eve BY, Bar-Eli M, Radinsky R, Dinney CP. Interleukin 8 expression regulates tumorigenicity and metastasis in human bladder cancer. *Cancer Res.* 2000; 60(8):2290–9. [PubMed: 10786697] (b) Ning Y, Manegold PC, Hong YK, Zhang W, Pohl A, Lurje G, Winder T, Yang D, LaBonte MJ, Wilson PM, Ladner RD, Lenz HJ. Interleukin-8 is associated with proliferation, migration, angiogenesis and chemosensitivity in vitro and in vivo in colon cancer cell line models. *Int J Cancer.* 2011; 128(9):2038–49. [PubMed: 20648559]
8. (a) Hagemann T, Lawrence T, McNeish I, Charles KA, Kulbe H, Thompson RG, Robinson SC, Balkwill FR. “Re-educating” tumor-associated macrophages by targeting NF-kappaB. *J Exp Med.* 2008; 205(6):1261–8. [PubMed: 18490490] (b) Shigeoka M, Urakawa N, Nakamura T, Nishio M, Watajima T, Kuroda D, Komori T, Kakeji Y, Semba S, Yokozaki H. Tumor associated macrophage expressing CD204 is associated with tumor aggressiveness of esophageal squamous cell carcinoma. *Cancer Sci.* 2013; 104(8):1112–9. [PubMed: 23648122]
9. Aref AR, Huang RY, Yu W, Chua KN, Sun W, Tu TY, Bai J, Sim WJ, Zervantonakis IK, Thiery JP, Kamm RD. Screening therapeutic EMT blocking agents in a three-dimensional microenvironment. *Integr Biol (Camb).* 2013; 5(2):381–9. [PubMed: 23172153]
10. Shao H, Yang B, Hu R, Wang Y. Matrine effectively inhibits the proliferation of breast cancer cells through a mechanism related to the NF-kappaB signaling pathway. *Oncol Lett.* 2013; 6(2): 517–520. [PubMed: 24137358]
11. Park SY, Jin ML, Kim YH, Lee SJ, Park G. Sanguinarine inhibits invasiveness and the MMP9 and COX2 expression in TPA-induced breast cancer cells by inducing HO-1 expression. *Oncol Rep.* 2014; 31(1):497–504. [PubMed: 24220687]
12. Dai F, Chen Y, Song Y, Huang L, Zhai D, Dong Y, Lai L, Zhang T, Li D, Pang X, Liu M, Yi Z. A natural small molecule harmine inhibits angiogenesis and suppresses tumour growth through activation of p53 in endothelial cells. *PLoS One.* 2012; 7(12):e52162. [PubMed: 23300602]
13. Pan X, Han H, Wang L, Yang L, Li R, Li Z, Liu J, Zhao Q, Qian M, Liu M, Du B. Nitidine Chloride inhibits breast cancer cells migration and invasion by suppressing c-Src/FAK associated signaling pathway. *Cancer Lett.* 2011; 313(2):181–91. [PubMed: 21959111]
14. Liu PL, Tsai JR, Charles AL, Hwang JJ, Chou SH, Ping YH, Lin FY, Chen YL, Hung CY, Chen WC, Chen YH, Chong IW. Resveratrol inhibits human lung adenocarcinoma cell metastasis by suppressing heme oxygenase 1-mediated nuclear factor-kappaB pathway and subsequently

- downregulating expression of matrix metalloproteinases. *Mol Nutr Food Res*. 2010; 54(Suppl 2):S196–204. [PubMed: 20461740]
15. Taniguchi S, Fujiki H, Kobayashi H, Go H, Miyado K, Sadano H, Shimokawa R. Effect of (-)-epigallocatechin gallate, the main constituent of green tea, on lung metastasis with mouse B16 melanoma cell lines. *Cancer Lett*. 1992; 65(1):51–4. [PubMed: 1511409]
 16. Li ZC, Zhang LM, Wang HB, Ma JX, Sun JZ. Curcumin inhibits lung cancer progression and metastasis through induction of FOXO1. *Tumour Biol*. 2013
 17. Huang YT, Hwang JJ, Lee PP, Ke FC, Huang JH, Huang CJ, Kandaswami C, Middleton E Jr, Lee MT. Effects of luteolin and quercetin, inhibitors of tyrosine kinase, on cell growth and metastasis-associated properties in A431 cells overexpressing epidermal growth factor receptor. *Br J Pharmacol*. 1999; 128(5):999–1010. [PubMed: 10556937]
 18. Shimizu K, Kinouchi Shimizu N, Hakamata W, Unno K, Asai T, Oku N. Preventive effect of green tea catechins on experimental tumor metastasis in senescence-accelerated mice. *Biol Pharm Bull*. 2010; 33(1):117–21. [PubMed: 20045947]
 19. Ho HH, Chang CS, Ho WC, Liao SY, Wu CH, Wang CJ. Anti-metastasis effects of gallic acid on gastric cancer cells involves inhibition of NF-kappaB activity and downregulation of PI3K/AKT/small GTPase signals. *Food Chem Toxicol*. 2010; 48(8–9):2508–16. [PubMed: 20600540]
 20. (a) De Stefano I, Raspaglio G, Zannoni GF, Travaglia D, Prisco MG, Mosca M, Ferlini C, Scambia G, Gallo D. Antiproliferative and antiangiogenic effects of the benzophenanthridine alkaloid sanguinarine in melanoma. *Biochem Pharmacol*. 2009; 78(11):1374–81. [PubMed: 19643088] (b) Basini G, Bussolati S, Santini SE, Grasselli F. Sanguinarine inhibits VEGF-induced angiogenesis in a fibrin gel matrix. *Biofactors*. 2007; 29(1):11–8. [PubMed: 17611290]
 21. Chen J, Wang J, Lin L, He L, Wu Y, Zhang L, Yi Z, Chen Y, Pang X, Liu M. Inhibition of STAT3 signaling pathway by nitidine chloride suppressed the angiogenesis and growth of human gastric cancer. *Mol Cancer Ther*. 2012; 11(2):277–87. [PubMed: 22203730]
 22. Jie S, Li H, Tian Y, Guo D, Zhu J, Gao S, Jiang L. Berberine inhibits angiogenic potential of Hep G2 cell line through VEGF down-regulation in vitro. *J Gastroenterol Hepatol*. 2011; 26(1):179–85. [PubMed: 21175812]
 23. Igura K, Ohta T, Kuroda Y, Kaji K. Resveratrol and quercetin inhibit angiogenesis in vitro. *Cancer Lett*. 2001; 171(1):11–6. [PubMed: 11485823]
 24. Chen Y, Li XX, Xing NZ, Cao XG. Quercetin inhibits choroidal and retinal angiogenesis in vitro. *Graefes Arch Clin Exp Ophthalmol*. 2008; 246(3):373–8. [PubMed: 18087712]
 25. Lu Y, Jiang F, Jiang H, Wu K, Zheng X, Cai Y, Katakowski M, Chopp M, To SS. Gallic acid suppresses cell viability, proliferation, invasion and angiogenesis in human glioma cells. *Eur J Pharmacol*. 2010; 641(2–3):102–7. [PubMed: 20553913]
 26. Tu TY, Wang Z, Bai J, Sun W, Peng WK, Huang RY, Thiery JP, Kamm RD. Rapid Prototyping of Concave Microwells for the Formation of 3D Multicellular Cancer Aggregates for Drug Screening. *Adv Healthc Mater*. 2013
 27. (a) Noe V, Willems J, Vandekerckhove J, Roy FV, Bruyneel E, Mareel M. Inhibition of adhesion and induction of epithelial cell invasion by HAV-containing E-cadherin-specific peptides. *J Cell Sci*. 1999; 112(Pt 1):127–35. [PubMed: 9841909] (b) Chen HF, Chuang CY, Lee WC, Huang HP, Wu HC, Ho HN, Chen YJ, Kuo HC. Surface marker epithelial cell adhesion molecule and E-cadherin facilitate the identification and selection of induced pluripotent stem cells. *Stem Cell Rev*. 2011; 7(3):722–35. [PubMed: 21305366]
 28. (a) Mendez MG, Kojima S, Goldman RD. Vimentin induces changes in cell shape, motility, and adhesion during the epithelial to mesenchymal transition. *FASEB J*. 2010; 24(6):1838–51. [PubMed: 20097873] (b) Fraga CH, True LD, Kirk D. Enhanced expression of the mesenchymal marker, vimentin, in hyperplastic versus normal human prostatic epithelium. *J Urol*. 1998; 159(1):270–4. [PubMed: 9400493]
 29. (a) Bersini S, Jeon JS, Dubini G, Arrigoni C, Chung S, Charest JL, Moretti M, Kamm RD. A microfluidic 3D in vitro model for specificity of breast cancer metastasis to bone. *Biomaterials*. 2014; 35(8):2454–61. [PubMed: 24388382] (b) Kamm RD, Bashir R. Creating Living Cellular Machines. *Ann Biomed Eng*. 2013(c) Jeon JS, Zervantonakis IK, Chung S, Kamm RD, Charest JL. In vitro model of tumor cell extravasation. *PLoS One*. 2013; 8(2):e56910. [PubMed: 23437268] (d) Zervantonakis IK, Hughes-Alford SK, Charest JL, Condeelis JS, Gertler FB, Kamm

RD. Three-dimensional microfluidic model for tumor cell intravasation and endothelial barrier function. *Proc Natl Acad Sci U S A*. 2012; 109(34):13515–20. [PubMed: 22869695]

**Figure 1.**

(A) Schematic illustration of the engineered microfluidic system for compound screening. Endothelial cells and cancer cell spheroids are applied to separate channels and co-cultured in their native 3D morphology in the tumor microenvironment. The device chamber is designed to allow diffusion of drugs and cell secretion. The two parallel gel channels in the middle are $600 \times 180 \mu\text{m}$ ($w \times h$) each, and the HUVEC/media channels by the side are $750 \times 180 \mu\text{m}$ ($w \times h$). (B) The inset photograph of 3D projection represents an intact endothelial monolayer at the interface between the collagen and HUVEC channels in the device. Immunofluorescent staining for VE-cadherin (green in the image), a surface marker for endothelial cells, was routinely performed in our study to verify the integrity of HUVEC monolayer. (C) A list of 12 compounds tested in this study.

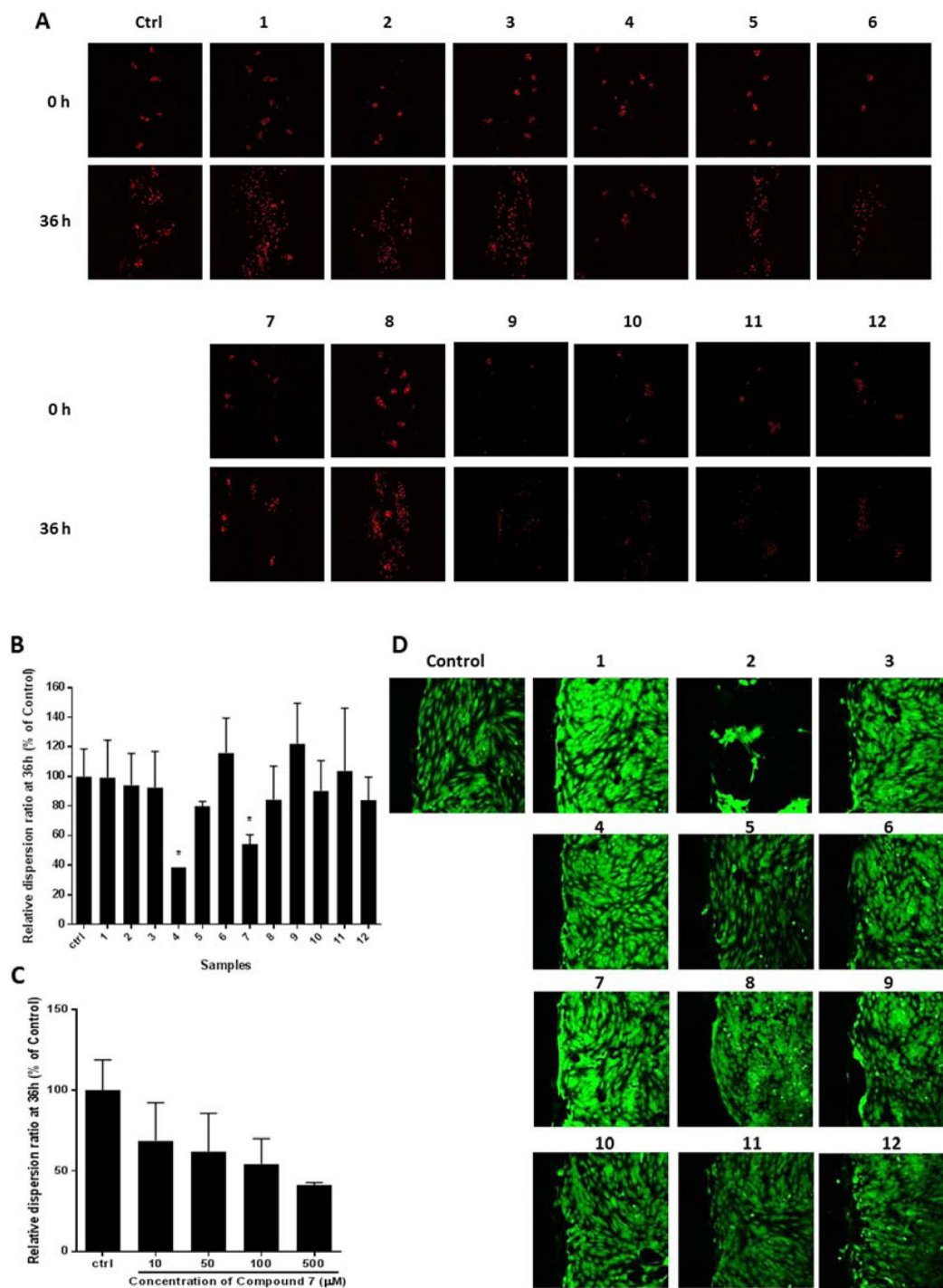


Figure 2.

(A) Representative images of A549 cancer spheroids before and after treatment with various compounds for 36 h. The cells were generated to stably express H2B-mCherry red fluorescence for visualization. (B) Quantitative analysis of the relative dispersion ratio of the spheroids. The relative dispersion rate of each sample group was determined and normalized to that in average of the control. Compounds 4 and 7 exhibited significant suppression of

spheroids dispersion. Data are expressed as Mean \pm S.D (n=4). * $P < 0.01$. (C) Comparison of the relative dispersion ratio of Compound 7 in different concentrations. (D) Representative images of the HUVECs pre-aligned along the channel after treatment with various compounds for 36 h (green for Calcein-AM staining), with Compound 2 causing obvious disruption to the endothelial layer.

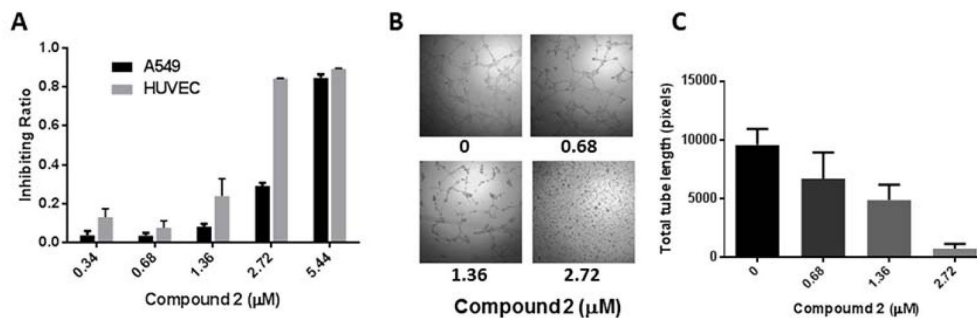


Figure 3.

(A) The inhibitory effect of Compound 2 (sanguinarine chloride hydrate) on the viability of A549 and HUVEC cells in monolayer culture. Data are shown as Mean \pm S.D (n=6). (B) Representative phase-contrast photographs of capillary tube formation of HUVECs on Matrigel and (C) Quantitative analysis of total tube length demonstrate that Compound 2 effectively inhibits tube formation in a dose-dependent manner. Data are shown as Mean \pm S.D (n=6).

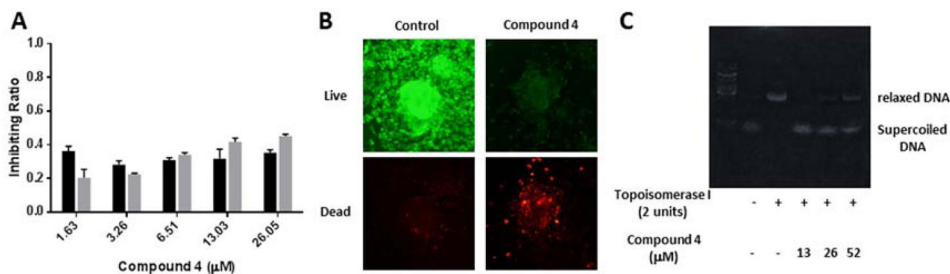


Figure 4. (A) The inhibitory effect of Compound 4 (nitidine chloride) on the viability of A549 and HUVEC cells in monolayer culture. Data are shown as Mean \pm S.D (n=6). (B) Representative images of fluorescent Live/Dead staining of A549 multicellular cancer aggregates (MCAs) incubated with or without 13 μM compound 4 after 24 h. (C) Representative photograph of agarose gel electrophoresis showing that Compound 4 inhibited the activity of Topoisomerase I in relaxing supercoiled DNA.

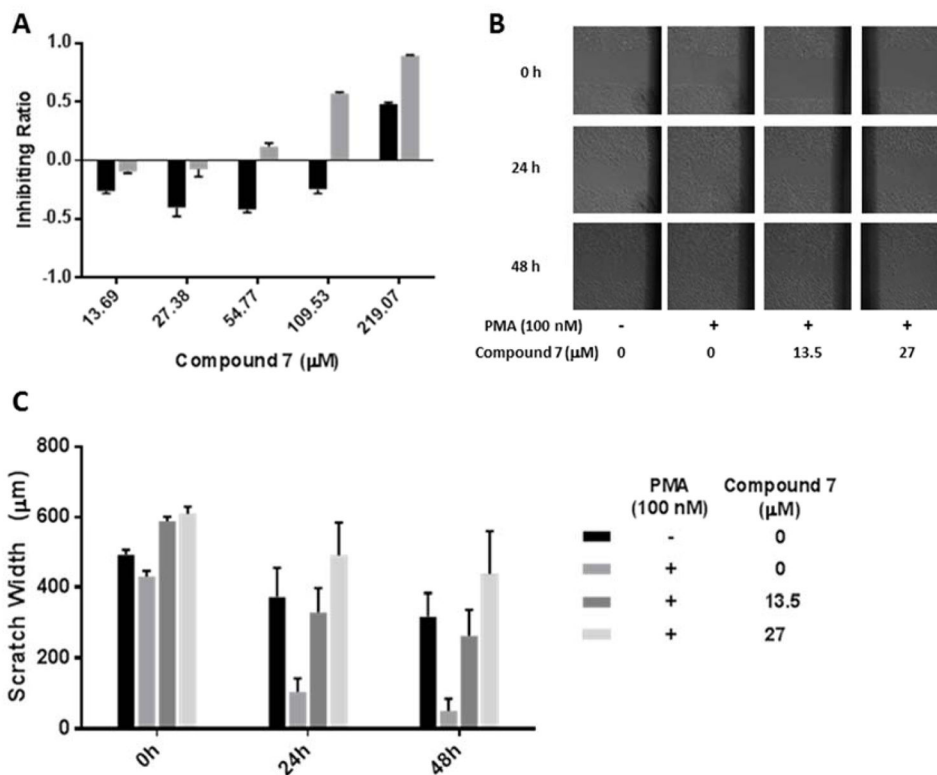


Figure 5. (A) The inhibitory effect of Compound 7 (resveratrol) on the viability of A549 and HUVEC cells in monolayer culture. Data are shown as Mean \pm S.D (n=6). (B) The inhibitory effects of Compound 7 on the migration of A549 cells, which in monolayer were scratched with a 200 μl pipette tip and then incubated with Compound 7 (13.5 or 27 μM) and PMA (100nM) for 24 and 48 h. Photos were taken using a phase-contrast microscopy. (C) Quantitation of the scratch width at 0, 24, and 48 h.